LETTER

Extreme multiphoton luminescence in GaAs

To cite this article: Evyatar Sabag *et al* 2016 *EPL* **115** 57006

A Letters Journal Exploring the Frontiers of Physics

September 2016

EPL, **115** (2016) 57006 www.epljournal.org
doi: 10.1209/0295-5075/115/57006

Extreme multiphoton luminescence in GaAs

Evyatar Sabag, Raja Marjieh and Alex Hayat[(a)]

Department of Electrical Engineering, Technion - Haifa 32000, Israel

received 23 July 2016; accepted in final form 21 September 2016
published online 17 October 2016

PACS 79.20.Ws – Multiphoton absorption
PACS 42.50.Hz – Strong-field excitation of optical transitions in quantum systems; multiphoton processes
PACS 78.55.Cr – III-V semiconductors

Abstract – We demonstrate experimentally extreme multiphoton-absorption cascades in GaAs. We show $(2+3)$- and $(2+4)$-photon luminescence, in which a two-photon transition occurs from the valence to the lower conduction band, followed by another 3- or 4-photon transition to the upper conduction band —inducing luminescence corresponding to several inter-band transitions in GaAs. Our systematic study of the observed effects verifies the cascaded multiphoton absorption, by monitoring the pump intensity and wavelength dependence of the observed luminescence spectra. The measurements are in good agreement with our modeling of multiphoton effects including Auger recombination. Our results open new directions in bulk-material band-structure exploration.

One of the most important concepts in solid-state physics is the energy band structure. A powerful modern technique widely used for band-structure studies is angle-resolved photoemission spectroscopy (ARPES) [1,2], in which electron momentum and energy are measured independently. Inverse photoemission is the reverse process [3,4], where an electron is injected into a high unoccupied energy band and the emitted photon resulting from the electron decay to lower energy band is measured. Both of these methods are key tools in understanding novel systems, such as topological insulators [5–7] and high-temperature superconductors [8–10]. Topological insulators have been shown to have surface band structure, which is entirely different from that of their bulk [11]. Such differences require experimental approaches capable of distinguishing bulk from surface states. Due to their relatively lower rates, multiphoton absorption processes result in larger penetration depth and thus occur mainly in the bulk of materials [12]. This attribute enables such multiphoton luminescence to serve as a complementary exploration tool to ARPES and inverse photoemission, which focus mainly on the surface band structure [13]. Moreover, multiphoton processes using low-energy photons allow much better energy resolution than that of high-energy photons used in conventional band-structure exploration methods. Two-photon processes in semiconductors have been studied extensively regarding the fundamental physics [14] including photonic structures [15,16] enhanced nondegenerate multiphoton absorption [17], as well as in practical applications [18]. Higher-order semiconductor multiphoton absorption is much less studied. Several works have shown three-photon absorption in semiconductors to be much weaker than two-photon absorption [12,19,20]. Nevertheless, three-photon absorption has been employed for practical multiphoton detection [21] and ultrafast pulse characterization [22,23]. Four-photon absorption observations in semiconductors are extremely rare [24] due to the small transition probabilities and the difficulty of eliminating competing processes in nonlinear transmission experiments. Three- and four-photon luminescence provide direct access to corresponding nonlinear absorption rates, and cascading such high-order nonlinear absorption can serve as a unique tool for semiconductor bulk band structure exploration. However, such high-order cascaded multiphoton luminescence and multiphoton transitions to higher conduction bands in semiconductors have not been observed before.

Here, we experimentally demonstrate extreme multiphoton-absorption–induced luminescence in GaAs. We observe multiphoton absorption intensity dependence by monitoring luminescence on several spectral lines corresponding to three different inter-band transitions in GaAs. By the investigation of pump wavelength and intensity dependence of all three spectral lines we confirm

[(a)]E-mail: alex.hayat@ee.technion.ac.il

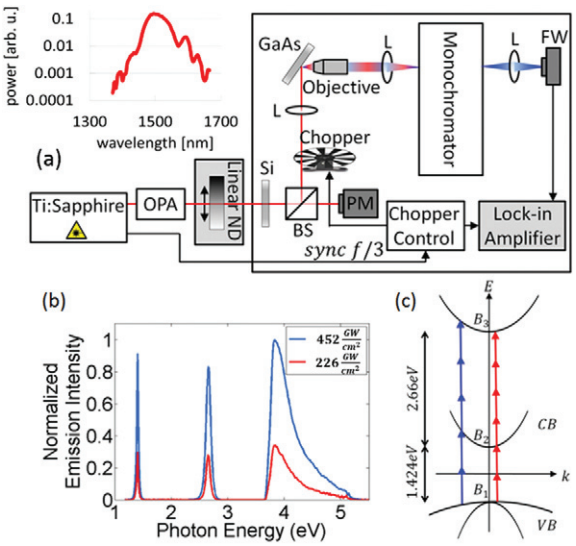

Fig. 1: (Colour online) (a) Experimental setup. The inset is the measured OPA pulse spectrum. (b) Measured spectral scan for 1500 nm pump for two pump intensities. (c) A diagram of GaAs energy bands, with the 2+3 (blue) and 2+4 (red) photon absorption processes.

the cascaded $2+3$ and $2+4$ multiphoton luminescence (fig. 1(c)).

In the observed cascades, the first step occurs in a two-photon inter-band absorption from the valence B_1 to conduction band B_2, whereas the second step occurs from the conduction band to a higher-energy band B_3 in a three-photon or four-photon transition —depending on the pump wavelength (fig. 1(c)). All observed cascaded nonlinearities exhibit saturation at high pump intensity limit. Furthermore, at the highest photon energy a surprising sharp increase in nonlinearity appears at pump intensities slightly below saturation. Our modelling shows that this nonlinearity increase results from the onset of Auger recombination at high charge-carrier density levels in the competing carrier decay path —confirmed by our measurements of the competing transition luminescence.

In our experiments, a 1 kHz Ti:Sapphire amplifier at 800 nm pumps our optical parametric amplifier (OPA). The OPA emission is tunable over a wide range of wavelengths from 500 nm to 2500 nm with extremely high peak powers (> 10 GW) and ~ 120 fs pulse duration. This extremely high intensity and tunability allows three- and four-photon absorption over a broad spectral range. In our experimental setup (fig. 1(a)) the intensity is controlled by a linear neutral density (ND) filter on a motorized stage, and the incident beam power is monitored by a sensitive thermal power meter (PM). A 1 mm thick Si wafer is used to eliminate undesired short-wavelength emission from the laser (shorter than 1000 nm). The pump beam is chopped at 333 Hz (to avoid harmonics of 50 Hz power grid frequency), synchronized to the laser repetition rate, and the resulting photoluminescence is detected by a femtowatt (FW) Si photoreceiver in a lock-in scheme.

In order to demonstrate multiphoton absorption, in the first experiment the pump wavelength was chosen at 1500 nm. The corresponding photon energy of $\sim$0.83 eV does not allow one-photon inter-band absorption in either $B_1 \to B_2$ or $B_2 \to B_3$ transitions with 1.42 eV or 2.66 eV energy differences, respectively, and it is almost 5 times smaller than the $B_1 \to B_3$ transition energy of 4.08 eV. In our photoluminescence measurements, however, all three spectral lines appear with 1500 nm pump wavelength —at energies of 1.42 eV, 2.66 eV and 4.08 eV, matching the $B_2 \to B_1$ luminescence, the $B_3 \to B_2$ luminescence and the $B_3 \to B_1$ luminescence, respectively (fig. 1(b)). The observed luminescence spectra are a result of a combination of several multiphoton transitions. For competing cascaded *vs.* direct multiphoton transitions the sum of photon energies in the process can be different. The range of photon energies corresponding to a specific B_1-to-B_3 cascaded transition is determined mainly by the density of states in the bands for transitions between finite crystal momentum k states. Therefore, the total transition energy can be larger than the zero-k B_1-B_3 energy gap. On the other hand, a competing direct B_1-to-B_3 multiphoton transition can occur at the zero-k B_1-B_3 energy gap with a smaller transition energy. Despite the different finite state energies for both processes, they contribute to the same time-averaged photoluminescence signal —after electron relaxation to the bottom of the B_3 band. At 1500 nm pump wavelength, the $B_1 \to B_2$ transition occurs by two-photon absorption, the $B_2 \to B_3$ transition can only occur by four-photon absorption, while the direct $B_1 \to B_3$ transition requires at least five-photon absorption and is thus not probable. Therefore, the observed lines are a signature of a cascaded $(2+4)$-photon absorption.

We conducted a systematic experimental study of the observed effects to verify the cascaded multiphoton absorption, by monitoring the intensity and pump wavelength dependence of the observed luminescence spectra. We modeled the expected dependence by rate-equation calculations to derive the intensity dependence of various multiphoton luminescence processes. Considering a three-band system, with N_i the occupation number of band B_i, we assumed the population of the higher conduction band B_3 to be much smaller than those of the other two bands $N_3 \ll N_1, N_2$ and we assumed the undepleted valence band B_1 population $\mathrm{d}N_1/\mathrm{d}t \to 0$. The rate equations for the combination of the nonlinear transitions considered here are

$$\begin{aligned} R_3 &= \frac{\mathrm{d}N_3}{\mathrm{d}t} = N_2 W_{23} + N_1 W_{13}, \\ R_2 &= \frac{\mathrm{d}N_2}{\mathrm{d}t} = (N_1 - N_2)\, W_{12} - N_2 W_{23} - \frac{N_2}{t_{sp}}, \\ R_1 &= \frac{\mathrm{d}N_1}{\mathrm{d}t} = 0, \end{aligned} \qquad (1)$$

where $N_3(0) = 0, N_2(0) = 0, W_{12}$, W_{23} and W_{13} are the transition rates between bands B_1-B_2, B_2-B_3 and B_1-B_3,

respectively, and are proportional to I_0^n, where I_0 is the incident pump intensity and n is the number of photons participating in the transition process. The selection rules between bands B_2 and B_3 are determined by the momentum matrix elements [25]. These matrix elements can in principle become identically zero for well-defined initial and final spin states. However, in our experiments, the initial and the finals states are spin degenerate, and both the three-photon and the four-photon transition have finite probabilities. The rates of both processes depend on the specific matrix element value as well as on the pump intensity. Our modeling is based on the phenomenological multiphoton rate equations [12], where the transition probabilities are proportional to the intensity to the power of the photon number, corresponding to the instantaneous multiphoton absorption. Some aspects of the cascaded multiphoton processes in our experiments are not fully described in the phenomenological model. More specifically, in our cascades the electron B_1-B_2 transition followed by the B_2-B_3 transition are coherent. The phase acquired by the electron in the B_1-B_2 step can be maintained before the second B_2-B_3 step, due to the ultrafast laser pulse duration. A more sophisticated semiconductor Bloch equation calculation can predict transition rates with better accuracy [26]. Nevertheless, the phenomenological model is sufficient to predict the power-law dependence of the different rates in our experiments.

The rate $\mathrm{d}N_3/\mathrm{d}t$ from the solution of the rate equations (eq. (1)) neglecting spontaneous emission during the short time of the pulse, and the transition probability from B_1 to B_3 W_{13} is

$$R_3 = \frac{\mathrm{d}N_3}{\mathrm{d}t} \approx \frac{N_1 W_{12} W_{23}}{W_{12} + W_{23}} \left[1 - e^{(-(W_{12}+W_{23})t)}\right]. \quad (2)$$

In the limit of the high peak intensity in our experiment, the rate takes a simpler form:

$$R_3 \approx \frac{N_1 W_{12} W_{23}}{W_{12} + W_{23}}. \quad (3)$$

A parallel process to consider is that of the $B_2 \rightarrow B_3$ charge carrier transition only, since at room temperature a certain concentration of charge carriers occupies the conductance band B_2. Assuming $N_3 \ll N_1, N_2$ the transition rate is

$$R_3 \approx N_2\,(0)\, W_{23} \quad (4)$$

with $N_2(0)$ the initial carrier number in band B_2. Here we assume the three- or four-photon transition to be weak enough so that $N_3 \ll N_2$.

To study the intensity dependence of the nonlinear luminescence, we set the pump to a shorter wavelength range (1200–1300 nm), where the observed luminescence spectral lines are much stronger due to possibility of the lower-order cascaded (2+3)-photon absorption. The measured intensity dependence for both spectral lines of the decay from the higher conduction band is the following: the $B_3 \rightarrow B_1$ and the $B_3 \rightarrow B_2$ transitions exhibiting

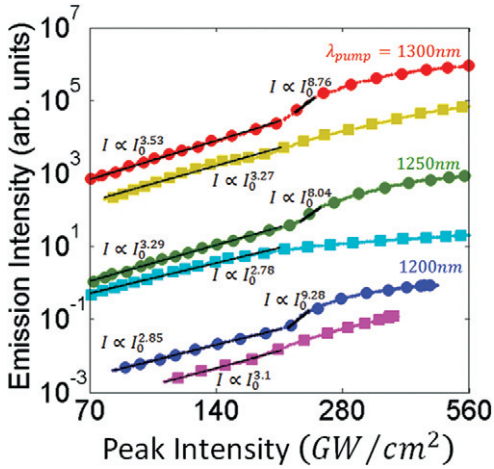

Fig. 2: (Colour online) (2 + 3)-photon absorption of shorter-wavelength pump (1200–1300 nm) absorption resulting in $B_3 \rightarrow B_2$ luminescence intensity (circles) and $B_3 \rightarrow B_1$ luminescence intensity (squares), *vs.* peak pump intensity for different wavelengths.

third-power dependence on the incident intensity (fig. 2). This dependence agrees well with the results of eqs. (3) and (4), this can be seen by taking the low-intensity limit of eq. (3) $W_{23} \ll W_{12}$:

$$R_3 \approx N_1 W_{23} \propto I_0^3 \quad (5)$$

which shows that the luminescence intensity is proportional to the third power of the pump intensity. This is in good agreement with our modelling which predicts the three-photon process to dominate the overall cascaded multiphoton absorption rate. The abrupt increase in pump intensity dependence around 250 GW/cm^2 not matching the expected dependence from our modeling of $I \sim I_0^3$ for the $B_3 \rightarrow B_2$ luminscence (fig. 2, circles) is attributed to the Auger recombination between the bands B_1 and B_2. This recombination reduces the population in band B_2, and thus increases the carrier decay probability from band B_3 to B_2 at the expense of the $B_3 \rightarrow B_1$ decay rate. The Auger recombination rate is proportional to the 3rd power of the carrier density and thus to I_0^6 due to the fact that the transition $B_1 \rightarrow B_2$ involves TPA. For higher pump intensities the dependence starts saturating due to filling of the electron density of states in the higher band and to emptying states in the lower band. The resulting general pump intensity dependence, not including the saturation, is

$$I_{out}^{n+m} \propto I_0^{n+m} \cdot \frac{a + bI_0^{3n}}{cI_0^n + dI_0^m}, \quad (6)$$
$$a > b, \quad c > d, \quad m > n.$$

The results for the longer wavelength range (1350–1500 nm) are also in good agreement (fig. 3) with our modelling in both eq. (3) and eq. (4) which predicts the four-photon process to dominate the overall cascaded multiphoton absorption rate.

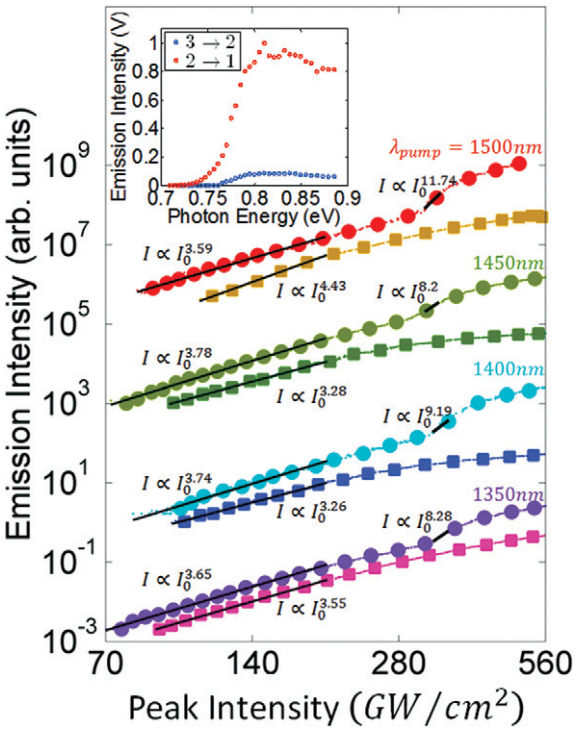

Fig. 3: (Colour online) (2 + 4)-photon absorption resulting in $B_3 \rightarrow B_2$ luminescence peak intensity (circles) and $B_3 \rightarrow B_1$ luminescence peak intensity (squares), *vs.* peak pump intensity for different wavelengths. Inset: two-photon absorption from B_1 to B_2 resulting in $B_2 \rightarrow B_1$ luminescence and (2+4)-photon absorption from B_1 to B_3 resulting in $B_3 \rightarrow B_2$ luminescence dependence on pump photon energy.

In order to distinguish which process dominates —the cascade process according to eq. (3) or direct B_2 to B_3 absorption with no cascade process according to eq. (4)— we examined the pump energy cut-off of the process at hand. We used a 1500 nm pump corresponding to the 4-photon $B_2 \rightarrow B_3$ transition. In the case of direct transition we would expect the minimal pump photon energy to be 2.66 eV/4 = 0.665 eV, whereas in our experiments the minimal energy is 0.75 eV (fig. 3, inset, blue markers). Looking at the $B_1 \rightarrow B_2$ theoretical 1.42 eV/2=0.71 eV energy cut-off and the experimental 0.72 eV energy cut-off (fig. 3, inset, red markers), it is clear that the four-photon process is directly dependent on the two-photon absorption (TPA) $B_1 \rightarrow B_2$, and only appears when the $B_1 \rightarrow B_2$ transition is strong enough in order to supply charge carriers to the transition $B_2 \rightarrow B_3$. Thus, the dominant process in our experiments is the $B_1 \rightarrow B_2 \rightarrow B_3$ cascade.

The sudden increase in pump intensity dependence around 300 GW/cm^2 in the four-photon case (fig. 3, circles), and around 250 GW/cm^2 in the three-photon case (fig. 2, circles) (not matching the expected dependence from eq. (3) of $I \sim I_0^3$ and $I \sim I_0^4$ for the $B_3 \rightarrow B_2$ luminescence) is attributed, as stated before, to the Auger recombination between the bands B_1 and B_2. The effect of the free-carrier response [27] in our experiment is negligible due to the low concentration of charge carriers in the excited conduction bands compared to the valence band as shown in the cut-off energy dependence (fig. 3, inset).

The finite bandwidth of the ultrafast pump pulse can in principle affect multiphoton transitions. In our experiments, the laser pulse duration is $\sim$ 120 fs with the corresponding spectral bandwidth of $\sim$ 30 meV ($\sim$ 60 nm at 1500 nm central wavelength). This finite range of photon energies, however, does not affect significantly the distinction between the different multiphoton transitions in our experiment due to the much larger scale of transition energies. For example, for 1500 nm (0.83 eV) pump photons, the dominant transition between bands B_2 and B_3 with a 2.66 eV energy gap is the four-photon absorption. In principle, however, some probability exists of a lower-order 3-photon transition between B_2 and B_3, due to the finite bandwidth of the laser pulse. Nevertheless, the intensity at the corresponding photon energy of 0.88 eV (1400 nm) is 2 orders of magnitude lower than the one at the central wavelength (fig. 1(a), inset), thus reducing the probability of three-photon absorption by 6 orders of magnitude. In contrast, the measured four-photon absorption at the intensity levels used in our experiments is only 1–2 orders of magnitude smaller than three-photon absorption —at the central laser wavelength. Therefore, at 1500 nm in our experiments, the four-photon absorption at the central wavelength is significantly more dominant than the possible three-photon absorption of the pulse component at 1400 nm —far from the central wavelength. This is verified by the measured intensity dependence power laws (figs. 2, 3).

In conclusion, we have provided experimental evidence for extreme multiphoton-absorption–induced luminescence in GaAs. We verified the (2+3)- and (2+4)-photon absorption in GaAs by the investigation of the pump wavelength and intensity dependence matching our calculation. Our results enable multiphoton-based bulk energy band-structure studies with finer energy resolution than that of linear processes.

REFERENCES

[1] Damascelli A., Hussain Z. and Shen Z. X., *Rev. Mod. Phys.*, **75** (2003) 473.
[2] Hermanson J., *Solid State Commun.*, **22** (1977) 9.
[3] Dose V., *Surf. Sci. Rep.*, **5** (1985) 337.
[4] Binnig G., Frank K. H., Fuchs H., Garcia N., Reihl B., Rohrer H., Salvan F. and Williams A. R., *Phys. Rev. Lett.*, **55** (1985) 991.
[5] Xia Y., Qian D., Hsieh D., Wray L., Pal A., Lin H., Bansil A., Grauer D. H. Y. S., Hor Y. S., Cava R. J. and Hasan M. Z., *Nat. Phys.*, **5** (2009) 398.
[6] Moore J. E., *Nature*, **464** (2010) 194.
[7] Hasan M. Z. and Kane C. L., *Rev. Mod. Phys.*, **82** (2010) 3045.
[8] Lanzara A., Bogdanov P. V., Zhou X. J., Kellar S. A., Feng D. L., Lu E. D., Yoshida T., Eisaki H.,

Fujimori A., Kishio K. and Shimoyama J. I., *Nature*, **412** (2001) 510.
[9] Dagotto E., *Rev. Mod. Phys.*, **66** (1994) 763.
[10] Timusk T. and Statt B., *Rep. Prog. Phys.*, **62** (1999) 61.
[11] Chen Y. L., Analytis J. G., Chu J. H., Liu Z. K., Mo S. K., Qi X. L., Zhang H. J., Lu D. H., Dai X., Fang Z. and Zhang S. C., *Science*, **325** (2009) 178.
[12] Nathan V., Mitra S. S. and Guenther A. H., *J. Opt. Soc. Am. B*, **2** (1985) 294.
[13] Plummer E. W. and Eberhardt W., *Angle-Resolved Photoemission as a Tool for the Study of Surfaces* (John Wiley & Sons, Inc.) 2007, pp. 533–656.
[14] Ota Y., Iwamoto S., Kumagai N. and Arakawa Y., *Phys. Rev. Lett.*, **107** (2011) 233602.
[15] Wagner S., Helmy A. S., Hutchings D. C. and Aitchison J. S., *J. Opt. Soc. Am. B*, **24** (2007) 1557.
[16] Poddubny A. N., Ginzburg P., Belov P. A., Zayats A. V. and Kivshar Y. S., *Phys. Rev. A*, **86** (2012) 033826.
[17] Cirloganu C. M., Padilha L. A., Fishman D. A., Webster S., Hagan D. J. and Van Stryland E. W., *Opt. Express*, **19** (2011) 22951.
[18] Hayat A., Nevet A., Ginzburg P. and Orenstein M., *Semicond. Sci. Technol.*, **26** (2011) 083001.
[19] Mitra S. S., Judell N. H. K., Vaidyanathan A. and Guenther A. H., *Opt. Lett.*, **7** (1982) 307.
[20] Kang J. U., Villeneuve A., Sheik-Bahae M., Stegeman G. I., Al-hemyari K., Aitchison J. S. and Ironside C. N., *Appl. Phys. Lett.*, **65** (1994) 147.
[21] Nevet A., Hayat A. and Orenstein M., *Opt. Lett.*, **36** (2011) 725.
[22] Langlois P. and Ippen E. P., *Opt. Lett.*, **24** (1999) 1868.
[23] Streltsov A. M., Moll K. D., Gaeta A. L., Kung P., Walker D. and Razeghi M., *Appl. Phys. Lett.*, **75** (1999) 3778.
[24] Hasselbeck M. P., Van Stryland E. W. and Sheik-Bahae M., *J. Opt. Soc. Am. B*, **14** (1997) 1616.
[25] Flatté M. E., Young P. M., Peng L.-H. and Ehrenreich H., *Phys. Rev. B*, **53** (1996) 1963.
[26] Koch S. W., Peyghambarian N. and Lindberg M., *J. Phys. C: Solid State Phys.*, **21** (1988) 5229.
[27] Ginzburg P., Krasavin A. V., Wurtz G. A. and Zayats A. V., *ACS Photon.*, **2** (2015) 8.